

Fermi National Accelerator Laboratory

FERMILAB-Conf-76/67-EXP
7100.317

COHERENT ELASTIC AND INELASTIC SCATTERING
FROM DEUTERIUM AND HELIUM

Ernest Malamud
Fermi National Accelerator Laboratory, Batavia, Illinois

July 1976



FERMILAB-Conf-76/67-EXP

COHERENT ELASTIC AND INELASTIC SCATTERING
FROM DEUTERIUM AND HELIUM

Ernest Malamud

Talk presented at the Topical Meeting on Multiparticle
Production on Nuclei at Very High Energy
Trieste, Italy, June 10-15, 1976

COHERENT ELASTIC AND INELASTIC SCATTERING
FROM DEUTERIUM AND HELIUM*

Joint Institute for Nuclear Research (Dubna, USSR)-
University of Arizona (Tucson, Arizona)-Fermilab
(Batavia, Illinois)-University of Rochester (Rochester,
New York)-Rockefeller University (New York, New York)
Collaboration.

Presented by Ernest Malamud
Fermilab, Batavia, Illinois 60510 - U.S.A.

In this talk I will review some of the past results and current plans of the Dubna-U.S.A. collaboration working in the Internal Target Area at Fermilab. This collaboration started in 1972 and has been engaged in a continuous series of experiments, all of which use the same basic technique of the circulating beam of the accelerator making multiple traversals of a thin target and recoil detection by means of solid state detectors.¹⁾ The important physics advantages of this technique are:

(1) very thin targets ($\sim 10^{-7}$ gm/cm²) are used so low $|t|$ recoils can be studied,

(2) there is a continuous sweep in incident energy from 8 GeV to the accelerator maximum (500 GeV at present; will be increased in the future to 1000 GeV with the Energy Doubler/Saver) so the s-dependence of quantities of interest is determined,

(3) the beam target intersection region is small, less than 1 cm, so the experiments benefit from point target geometry.

The reactions studied are of the type



where $A = p, d, \text{ or } \alpha$ and where M_x either equals m_p (elastic) or is greater (inelastic).

The specific experiments past, present, and future are summarized in Table I:

TABLE I
Dubna-USA Internal Target Experiments

Fermilab Number	Status	Reactions	$ t $ -range (GeV/c) ²	M_x -range	Target- Detector distance (m.)
36	Complete	pp elastic	.001-.09		2.5
186	Complete	pp elastic, inelastic	.013-.14	<40 GeV ²	2.5
317	Analysis in progress	pp,pd inelastic	<.2	<100 GeV ²	1.5
381	Future	pp,pd elastic, inelastic			7.5
289	Future	pHe ⁴ elastic, inelastic		(uses quadrupole focussing)	5.5

In all the reactions listed only the coherently recoiling nucleon or nucleus is detected; thus measurements are made either of elastic scattering or inclusive inelastic reactions of the type where the incident proton undergoes diffraction dissociation. Although the basic aim in this work is to learn more about the nucleon-nucleon interaction, nuclear targets have certain advantages: (1) enhancement of the small angle (low- t) cross sections due to coherence, (2) improvement of signal/background ratios, (3) He⁴ is a spin = 0 target.

I. The Fermilab Internal Target Area

The Internal Target Area, shown in Fig. 1, is located in a long straight section (~ 50 meters) 1/3 of the way around the Fermilab Main Ring. Two types of thin targets are used for interactions with the circulating beam in the accelerator: (1) Rotating, (2) Gas "jet". The rotating target shown schematically in Fig. 2 consists of a wheel rotating at 60 cps on which are mounted thin filaments a few microns in diameter. These intersect the beam spot, typically 3-4 mm in size at high energies, and if they are

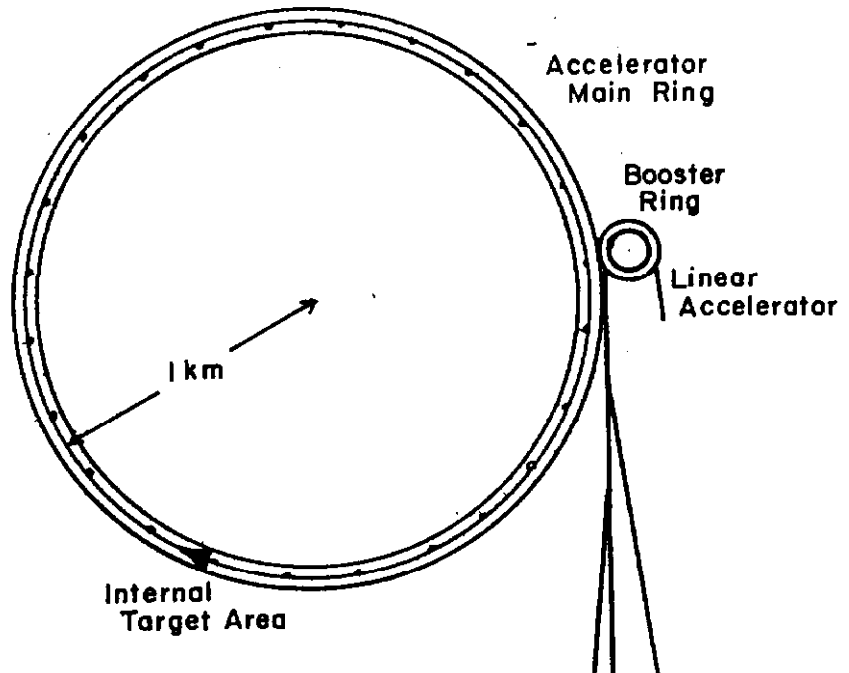


Fig. 1

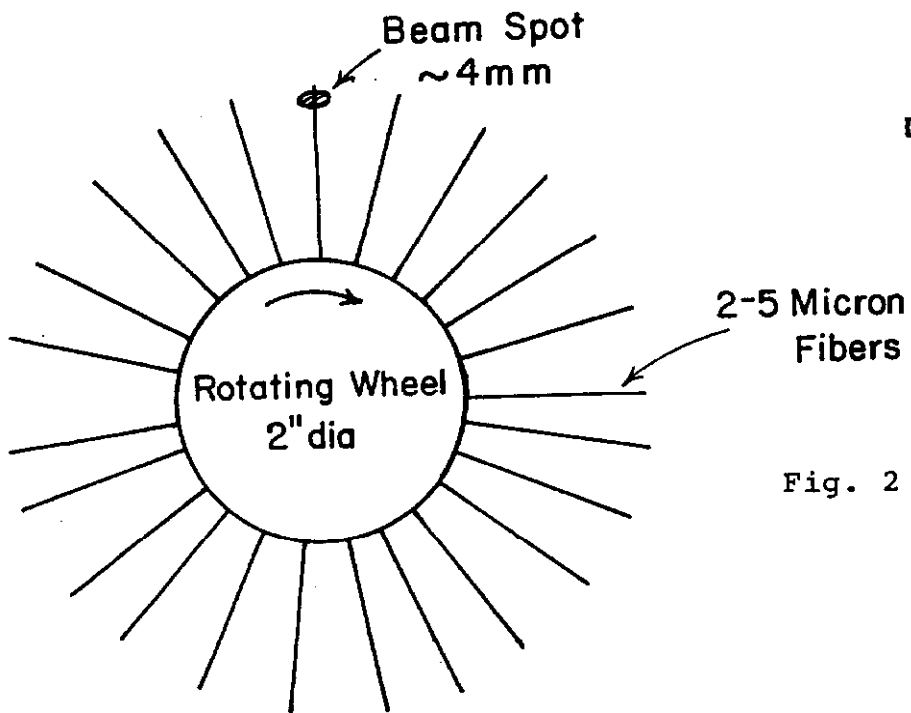
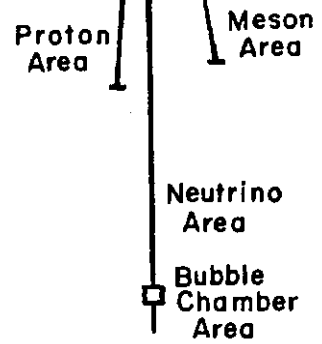


Fig. 2

spaced by this amount at the radius of intersection an almost D.C. spill can be obtained. Spokes of different materials can be mounted on the same wheel to obtain data from different nuclei during the same run. At one time it was possible to mount CH₂ foils and C filaments on the same wheel in order to obtain cross sections on hydrogen by subtraction.²⁾ This is no longer feasible because of the short life time of CH₂ foils at present beam intensities (1-2 x 10¹³ protons/pulse).

The target most commonly used at present in the Internal Target Area is the gas jet. There are two types: (1) the "cold" jet and (2) the "warm" jet. The cold jet, developed by the Dubna group³⁾ uses cryopumping by liquid helium. The warm jet,⁴⁾ in use now by two groups,^{5),6)} uses a large buffer volume to handle the pressure peak during the jet pulse. For operation of the cold jet with helium gas as a target, the cryopump has been coated with molecular sieve material to act as a buffer volume. A future experiment with the warm jet⁷⁾ will use target gases of Argon, Krypton, and Xenon.

The gas jet intersects the beam at 90° and at the point of intersection is 5 - 10 mm in diameter. The target density is adjustable. Typical operating luminosities are $\mathcal{L} \sim 10^{33} - 10^{34}/\text{cm}^2 \text{ sec}$. A schematic diagram of the Dubna-built cold jet is shown in Fig. 3. Cold hydrogen gas is pulsed through the de Laval nozzle, intersects the beam, and then is frozen in the liquid helium cooled cryotrap. When the cryotrap becomes full (after 2-3 hours of operation) the entire target assembly is remotely raised, the isolation valve to the main accelerator vacuum system closed and the accumulated hydrogen sublimated (takes about 45 minutes). The isolation valve can then be opened and the cycle repeated.

A layout of the Internal Target Area is shown in Fig. 4. In the first years of operation experimentation was confined to the 3 meter wide main ring tunnel. This hampered the use of magnetic analysis and limited the angular resolution

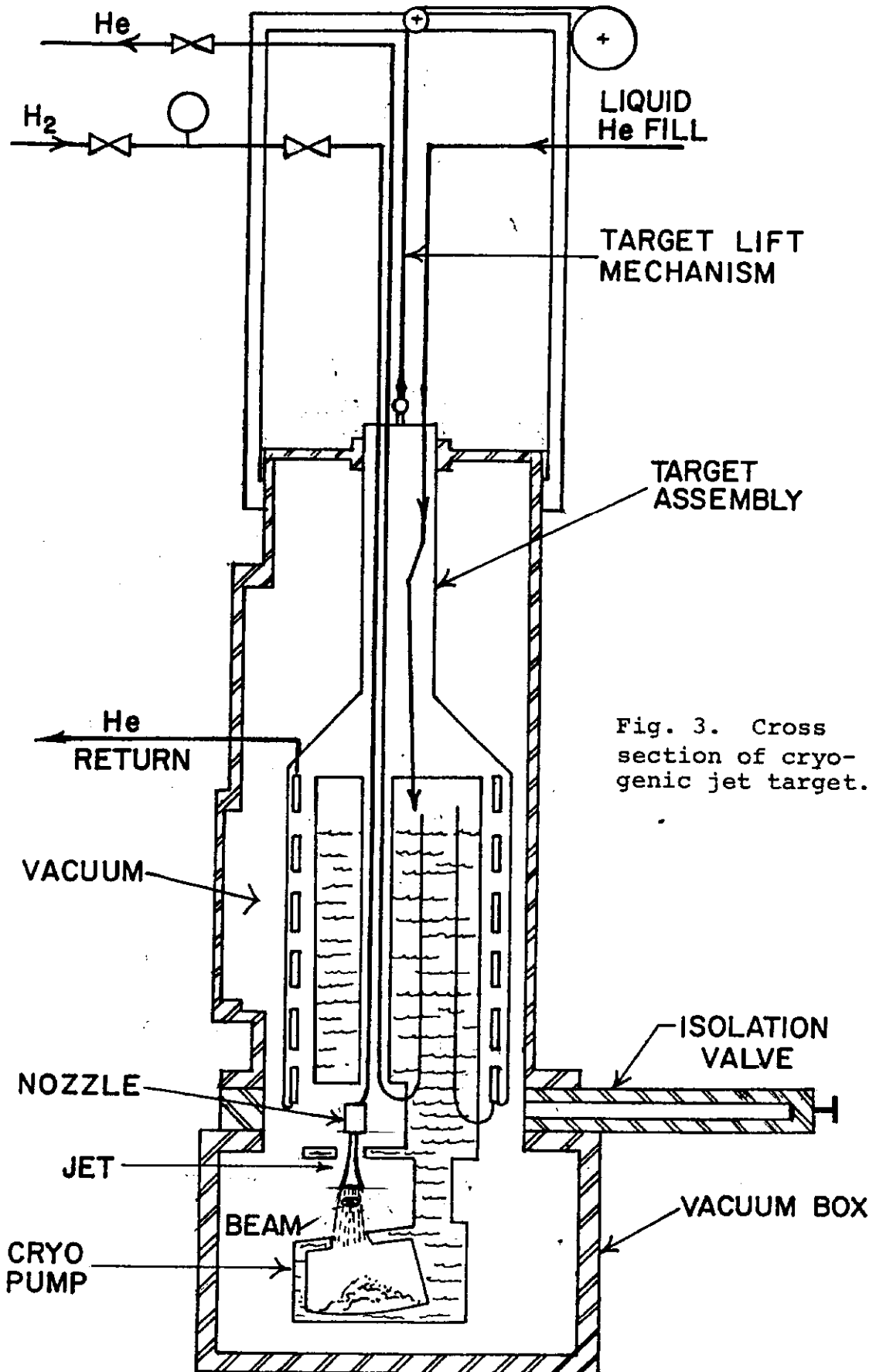


Fig. 3. Cross section of cryogenic jet target.

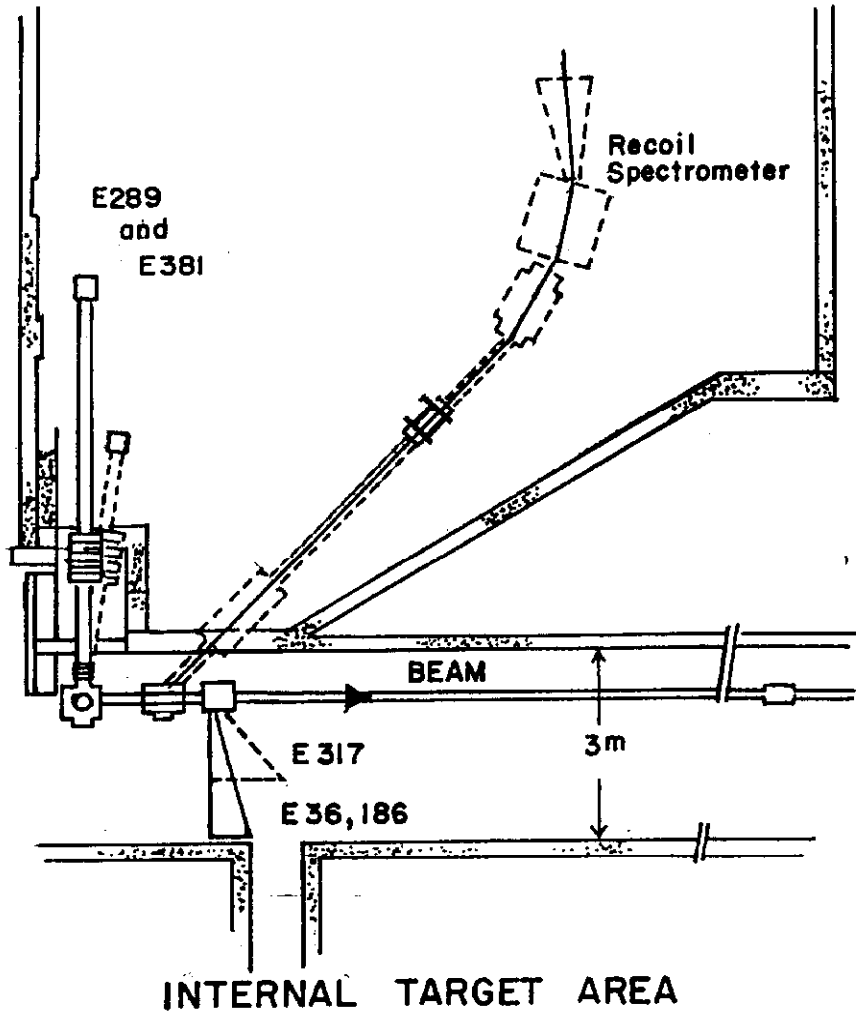


Fig. 4

attainable. A proposal⁸⁾ made in 1973 to enlarge the area was approved and in the spring of 1975 the large recoil room shown became available. The "ion guide", the vacuum box common to the accelerator vacuum system in which the recoils travel, can now be longer (5.5 - 7.5 m) for the future experiments (E-381, E-289) than in the past (E-36, E-186, E-317, 1.5 - 2.5 m). This increase of 3x to 5x in target-detector distance gives a corresponding decrease in ΔM_x , resolution in missing mass.

II. Dubna-U.S.A. Experiments in the Internal Target Area

The recoil kinematics of reactions (1) are described by

$$M_x^2 - m_p^2 = 2p|t|^{1/2} \left(\sin\omega - \frac{m_A+p}{2m_A p} |t|^{1/2} \right) \quad (2)$$

where p is the incident beam momentum and ω is the recoil angle measured from 90° in the laboratory. For elastic scattering the kinematics are almost independent of p ; thus, this is an ideal arrangement for measuring the s -dependence of such quantities as the slope parameter, b ,⁹⁾ or the ratio of the real to imaginary parts of the forward scattering amplitudes, ρ .¹⁰⁾ For inelastic scattering at fixed M_x^2 the separation from the elastic reaction becomes more difficult as p increases.

Surface barrier silicon detectors ranging from 25 μ to 5 mm in thickness are used to detect recoils. The standard technique of a dE/dx - E sandwich is used to separate different mass recoils. Figure 5 shows a scatter plot of the kinetic energies deposited in the front and back elements of the sandwich in a typical arrangement in the pd scattering experiment. The large accumulation of events at one place along the top branch is the pd elastic peak. There are three categories of events detected: (a) particles that stop in F, (b) particles that stop in B, and (c) particles that traverse both F and B. Category (c) as well as events too close to the "end point" are not used. As shown in Fig. 5 there is excellent mass separation for events in category (b). Elastic events in category (a) can also be used for physics by subtracting out the background under the elastic peak measured by shifting the detector to a different angle.

The detector stacks are placed on a movable carriage so for each event, after the mass separation has been done, there are three measured quantities: p , T , θ . Monitoring is done by a stack at fixed angle. Figure 6 shows a typical counting rate curve at fixed t as a function of recoil angle. The general "room" background as measured at an unphysical angle is small relative to the elastic peak. This level is apparently smaller with the cryopumped cold jet than with the warm jet. Nevertheless in the region of large missing mass it is an appreciable correction. In this region the backgrounds are measured by use of the anti-slit shown in Fig. 7. By blocking the direct path between target and detector one

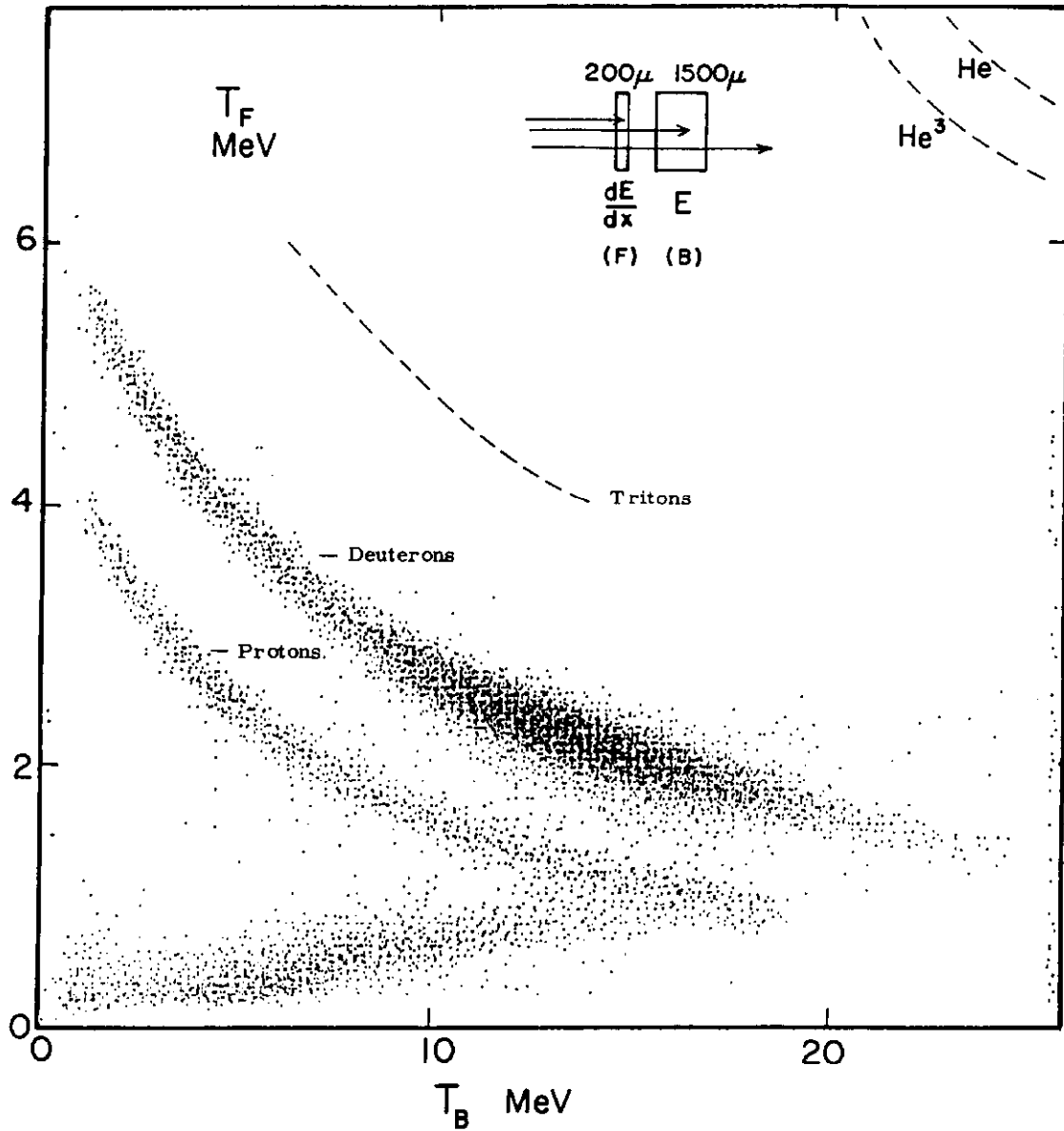


Fig. 5. Scatter plot of the pulse heights from front and back detectors in a typical pd scattering run.

COUNTING RATE VS ANGLE

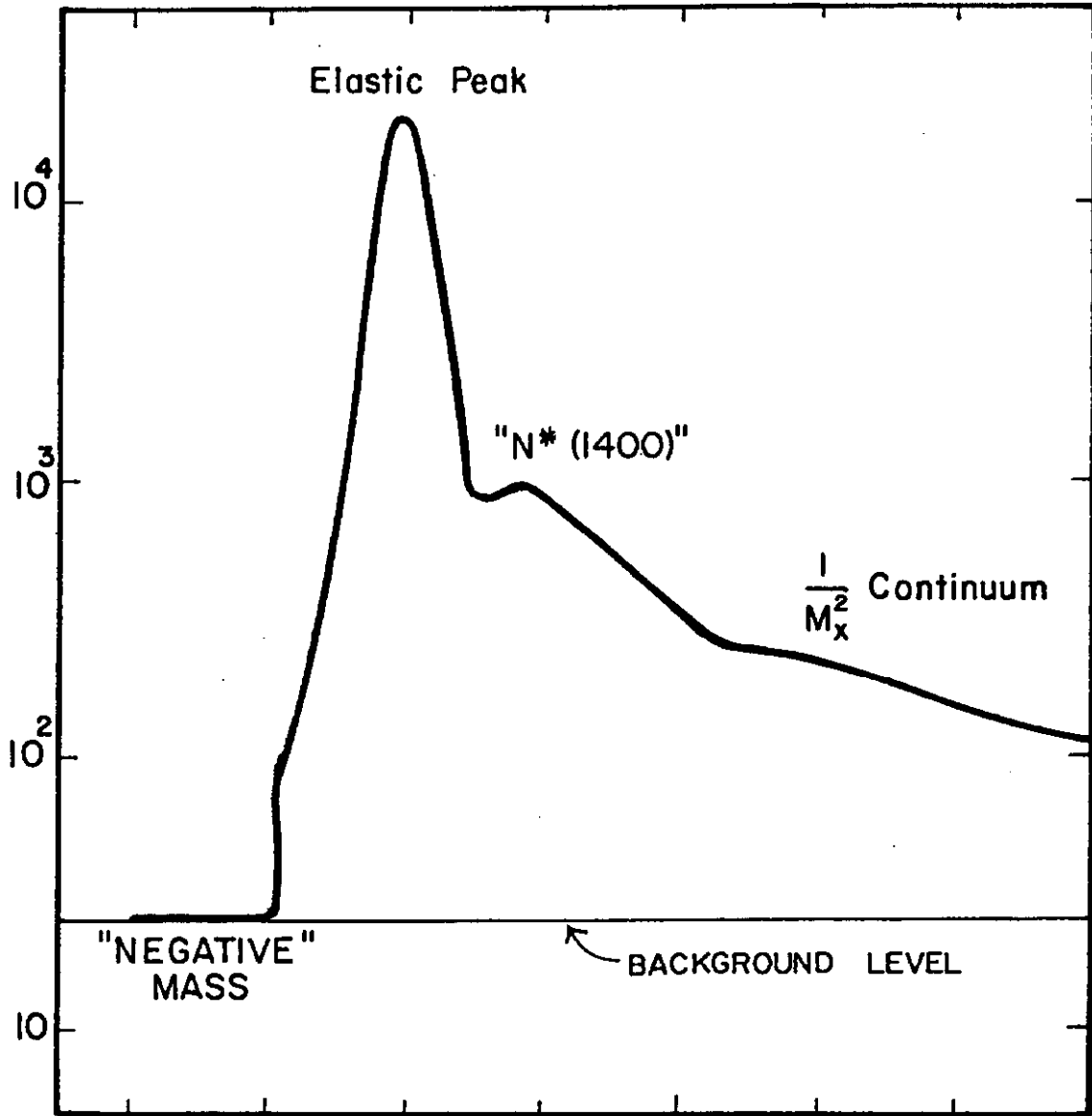


Fig. 6. Schematic curve of counting rate as a function of recoil angle at fixed p and t .

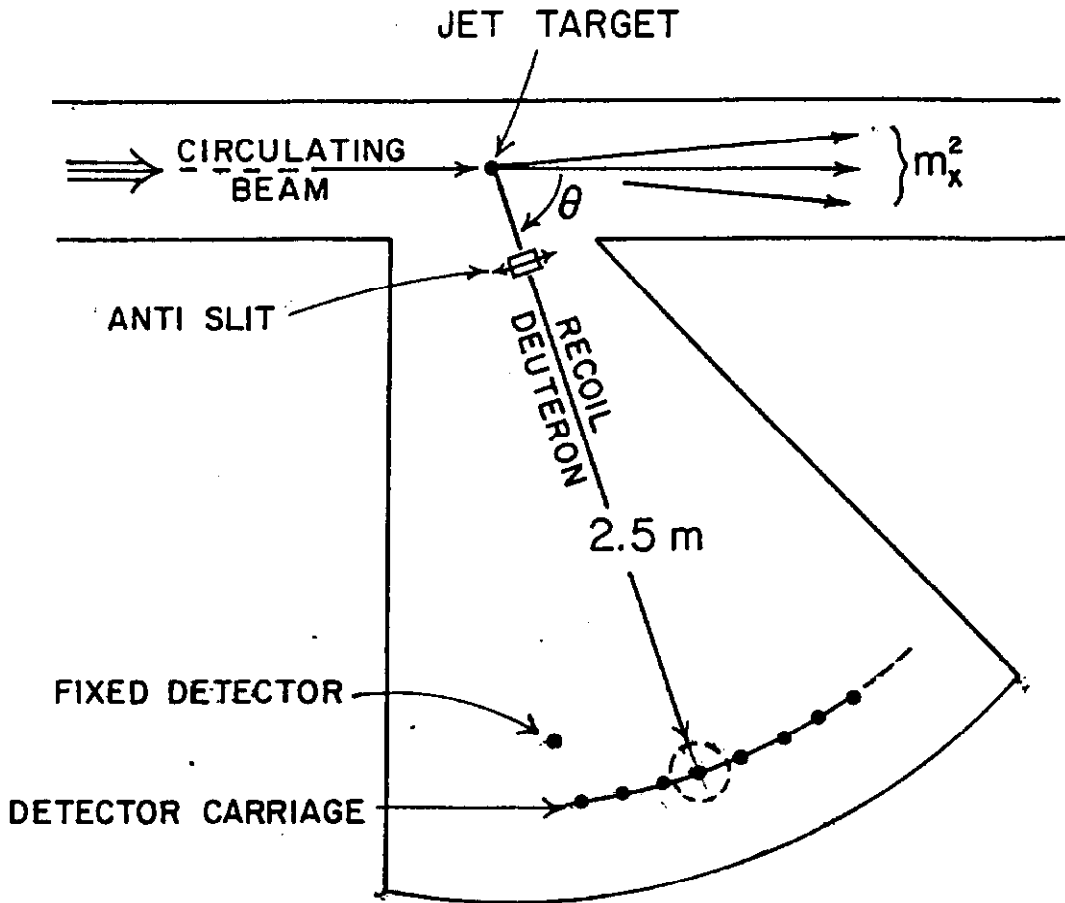


Fig. 7.

can measure the amount of elastic (or lower M_x^2) recoils scattered into the detector from the "wrong" angle. This background level is higher for recoil protons than for recoil deuterons. By studying and comparing inelastic scattering from both protons and deuterons we can increase our knowledge of the dynamics, since in the triple Regge region different amplitudes can contribute. For $M_x^2 \lesssim 0.1$ s where Pomeron exchange is expected to dominate both the pp and pd reactions the deuteron target can be used to obtain information on (beam) proton diffraction dissociation from protons. But for this method to work factorization must be valid.

III. Results on Factorization

The elastic pd cross section factorizes approximately as

$$\left(\frac{d\sigma}{dt}\right)^{pd} = \left(\frac{d\sigma}{dt}\right)^{pp} F_d(p,t) \quad (3)$$

where F_d is the coherence factor defined as

$$F_d(p, t) = \left[\frac{\sigma_t^{pd}(p)}{\sigma_t^{pp}(p)} \right]^2 \cdot |S(t)|^2 \quad (4)$$

In the momentum range of these experiments, $50 \leq p \leq 400$ GeV/c, $(\sigma_t^{pd}/\sigma_t^{pp})^2 = 3.6$ to better than 2%. In the region of small $|t|$ ($|t| < 0.12$ (GeV/c)²) the elastic pd data are reasonably well fit by the form factor

$$|S(t)|^2 = e^{b_0 t + ct^2} \quad (5)$$

and using coefficients measured in this work¹¹⁾

$$F_d(t) = 3.6 e^{26.4t + 62.3t^2} \quad (6)$$

Assuming that the inelastic cross-section factorizes in the same way as the elastic cross section, we can then obtain cross sections for the reaction $pp \rightarrow Xp$ by dividing the measured cross sections for $pp \rightarrow Xd$ by the elastic coherence factor.

$$\frac{d^2\sigma}{dt dM_x^2} (pd \rightarrow Xd) = \left[\frac{d^2\sigma}{dt dM_x^2} (pp \rightarrow Xp) \right] \cdot F_d(t) \quad (7)$$

One of the objectives of our experiments is to test this assumption over a range of p , t , and M_x . If Glauber-type corrections are comparable to those for elastic scattering ($\lesssim 10\%$) this procedure is expected to yield correct values for $pp \rightarrow Xp$ including the measurement of b to $\sim 10\%$.

Published results from E-186¹²⁾ have been used to test factorization.¹³⁾ Figure 8 reproduced from Ref. 13 compares $pp \rightarrow Xp$ cross sections at $p = 275$ GeV/c extracted from deuterium data using (7) with other measurements directly on protons. The cross sections are all reduced to the same value of $|t|$ by extrapolation using the measured slope parameters. The striking agreement shows that factorization can be used successfully to obtain nucleon cross sections from deuterium. Figure 8 shows a prominent peak at $M_x^2 = 1.9$ GeV², (the so called N*(1400) region) as well as less

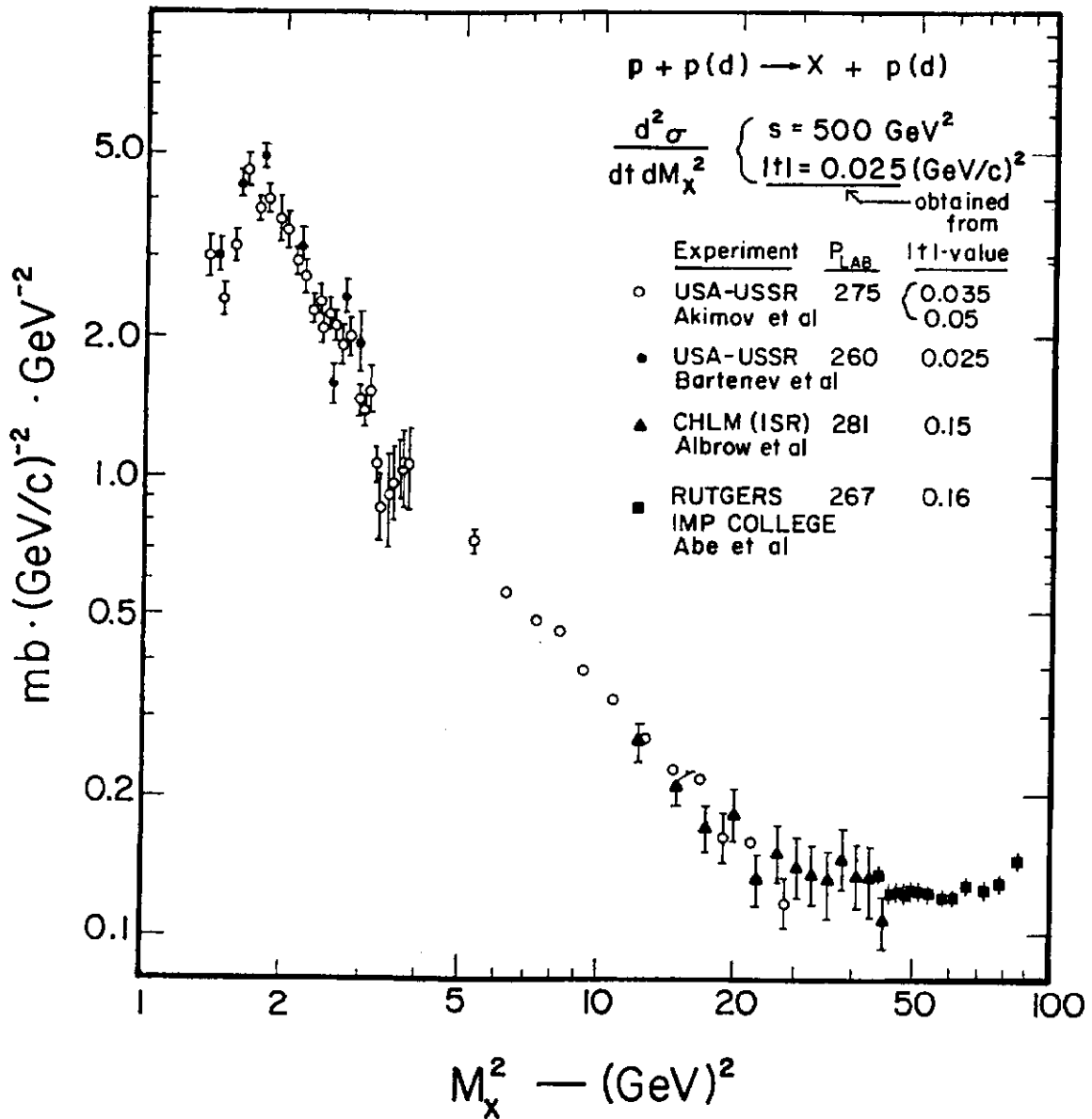


Fig. 8. Compilation of measurements on pp inelastic scattering and pd inelastic scattering with the coherence factor divided out. The figure is taken from Ref. 13 where references to the individual experiments are given.

obvious structure at 2.8 GeV^2 ($N^*(1688)$). Figure 9, taken from Ref. 14, is another illustration of factorization. This figure shows the agreement in the cross section for the $N^*(1400)$ enhancement obtained directly in pp collisions and indirectly by factorization from pd interactions.

The fits to the extracted cross sections discussed in detail in Ref. 13 can be summarized as follows. An adequate fit of the differential cross section is given by

$$\frac{d^2\sigma}{dt dM_x^2} = \frac{A \left(1 + \frac{B}{p_{\text{Lab}}}\right)}{M_x^2} b_0 e^{b_0 t} \quad (8)$$

$$A = 0.54 \pm 0.02 \text{ mb}$$

$$B = 54 \pm 16 \text{ GeV/c}$$

$$b_0 = 6.5 \pm 0.3 \text{ (GeV/c)}^{-2}$$

where the uncertainties include a $\pm 3\%$ normalization uncertainty. As M_x^2 decreases b increases by almost a factor of 4 to a maximum at $M_x^2 \approx 1.9 \text{ GeV}^2$. It is remarkable that this formula also describes the average behavior of the cross section in the resonance region if b_0 is replaced by $b(M_x^2)$.

If we integrate (8) over t we obtain:

$$\frac{A}{M_x^2} \left(1 + \frac{B}{p_{\text{Lab}}}\right) \rightarrow \frac{A}{M_x^2} \quad (9)$$

as $p_{\text{Lab}} \rightarrow \infty$

An integration over missing mass¹⁵⁾ yields:

$$\sigma_{\text{Diff}} = 2 \int_{\text{threshold}}^{\text{max}} \frac{A}{M_x^2} dM_x^2 = 2A \ln s + \text{constant} \quad (10)$$

$$\sigma_{\text{Diff}} \approx 1.1 \ln s (\text{mb}) + \text{constant}$$

where the factor of two is, of course, to account for target diffraction as well as beam diffraction. The total double diffractive cross section has been measured recently at the ISR by the UCLA-Saclay collaboration.¹⁶⁾ If their result is used and it is assumed that the M_x^2 dependence is the same for double and single diffraction, then the coefficient in

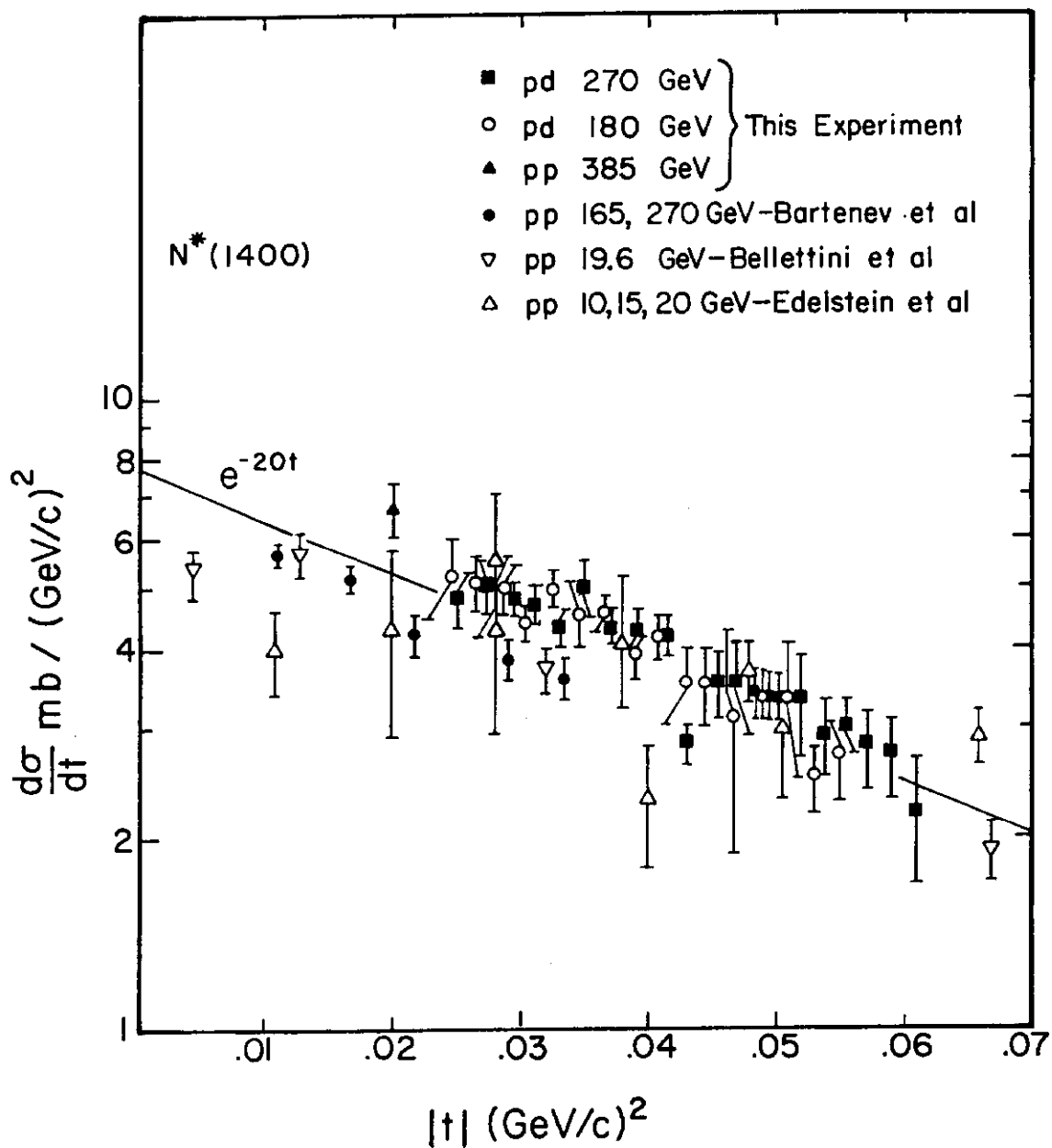


Fig. 9. Compilation of inelastic cross sections in the " $N^*(1400)$ " region taken from pp data and from pd data divided by the coherence factor. The figure is taken from Ref. 14 where references to the individual experiments are given.

(10) is increased to about 1.7. The coefficient obtained is of the right order of magnitude to ascribe the increase in σ_t^{pp} to diffractive processes.¹⁷⁾

IV. Some Elastic Scattering Results

Figure 10 shows the "transparency", $\sigma_{\text{elastic}}/\sigma_{\text{total}}$, for pp and pd scattering as a function of incident momentum. The pp data in Fig. 10a are from Ref. 18 and the pd data in Fig. 10b from Ref. 11. The normalization shift in the two sets of data shown in Fig. 10b is due to different assumptions about the high- $|t|$ (unmeasured) contribution to σ_{el} . This normalization difference is eliminated if the high- $|t|$ contribution for the high energy data set is calculated in the same manner as was done for the lower energy data set. Both pp and pd data appear to saturate at high energy supporting a geometrical scaling hypothesis. The smaller value in the pd case indicates a greater transparency of the scattering disk.

Now I want to discuss a problem in pd elastic scattering. The slope parameter or radius of interaction, b , is one of the fundamental parameters used to describe the strong interaction. It is a well known result from the Dubna-U.S.A. collaboration⁹⁾ that in pp collisions b is given by

<p><u>pp elastic</u></p> <p>$P_{\text{Lab}} > 100 \text{ GeV/c}$</p> <p>$.005 \leq t \leq .09 \text{ (GeV/c)}^2$</p> <p>$b = b_0 + 2\alpha' \ln s/s_0 \quad s_0 = 1 \text{ GeV}^2$</p> <p>$b_0 = 8.23 \pm 0.27 \text{ (GeV/c)}^{-2}$</p> <p>$\alpha' = 0.278 \pm 0.024 \text{ (GeV/c)}^{-2}$</p>

A less well known result is our measurement of "shrinkage", α' , on deuterons.¹¹⁾

<p><u>pd elastic</u></p> <p>$50 < P_{\text{Lab}} < 400 \text{ GeV/c}$</p> <p>$.013 \leq t < 0.14 \text{ (GeV/c)}^2$</p> <p>$b = b_0 + 2\alpha' \ln s/s_0 \quad s_0 = 1 \text{ GeV}^2$</p> <p>$\alpha' = 0.47 \pm 0.02 \text{ (GeV/c)}^{-2}$</p>

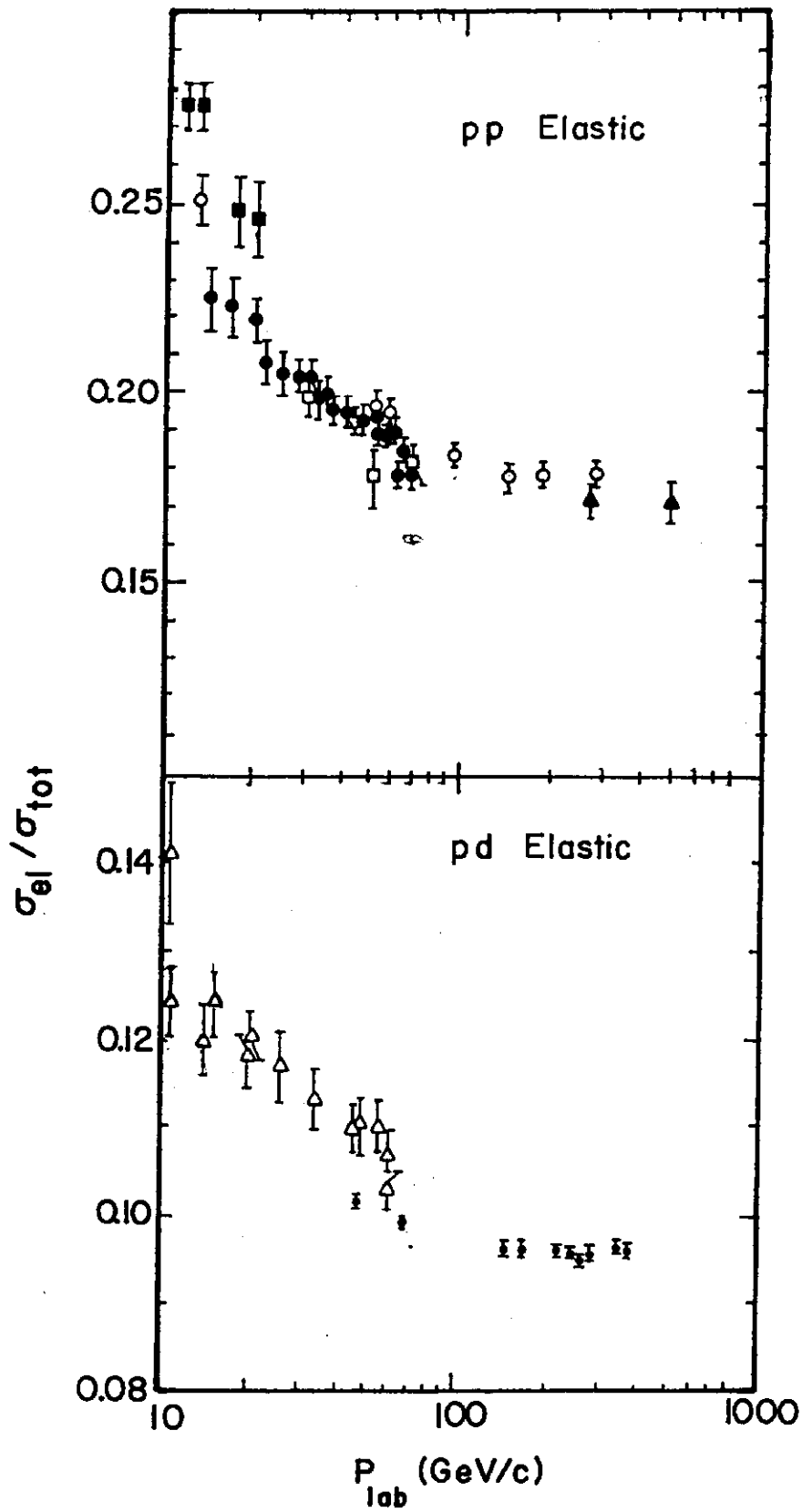


Fig. 10(a)

Fig. 10(b)

Fig. 10(a) σ_{el}/σ_{tot} for pp scattering (b) σ_{el}/σ_{tot} for pd scattering. (a) is taken from Ref. 18 and (b) from Ref. 11. See those references for references to the individual experiments.

The pd result comes from a fit to 225 data points at 12 different energies. In pd scattering b_0 is difficult to determine because of the correlation with the deuteron form factor but α'_{pd} is believed to be reliable. Does $\alpha'_{pd} \neq \alpha'_{pp}$ mean a difference between neutron and proton? If pn elastic scattering is extracted using "Glauber theory" then $\alpha'_{pn} = 0.58 \pm 0.05 \text{ (GeV/c)}^{-2}$. But there are several problems with this determination:

(1) The t dependence of ρ (the ratio of the real to imaginary part of the nucleon-nucleon scattering amplitude) is unknown in our energy range.

(2) The fit which yielded the value of α'_{pn} above neglected d-wave.

(3) The inelastic double scattering was not included.

Nothing can be done about problem (1) except to assume $\rho(t)$ is independent of t until measurements have been done (see Section V). The complete differential cross section in terms of the s- and d-wave single and double scattering amplitudes can be written:

$$\begin{aligned} \frac{d\sigma}{dt} = & \left| S_0\left(\frac{t}{4}\right) (A_c + A_p + A_n) + A_{G_s} \right|^2 & (11) \\ & + \frac{1}{4} \left| S_2\left(\frac{t}{4}\right) (A_p + A_n) + A_{G_d} \right|^2 \\ & + \frac{3}{4} \left| S_2\left(\frac{t}{4}\right) (A_p + A_n) \right|^2 \end{aligned}$$

The α'_{pn} value obtained above neglected the second and third terms in (11) and there are too many parameters to use our data alone to determine them. These terms become relatively more important as $|t|$ increases; at $|t| = 0.10$ they make a 4% contribution. If our data is refit using a fixed d-wave contribution the effect on b_{pn} is less than 10%. Finally the inelastic Glauber correction can be included by writing

$$A_{G_s} = A_{G_{el}} + A_{G_{inel}}. \quad (12)$$

If $A_{G_{inel}}$ is evaluated using our own inelastic data then we obtain values of α'_{pn} ranging from 0.35 to 0.57 due to the

uncertainty in $A_{G_{inel}}$ but showing that equality of α'_{pn} and α'_{pp} may be found by the correct inclusion of the inelastic Glauber correction. A recent calculation by Ya. I. Azimov et al.¹⁹⁾ does indeed obtain agreement with our measurement of α'_{pd} by using a larger energy dependence in $A_{G_{inel}}$.

V. Future Dubna-USA Experiments

E-381 and E-289 share a common apparatus, a 7.5 m long ion guide constructed almost equally from parts made in the U.S. and the U.S.S.R. The layout is shown in Fig. 4. As of this date all the components are in place and data taking is ready to start. The new setup is superior to the equipment used in E-36, E-186 and E-317 in the following respects: (1) It extends through a hole in the straight section into the new experimental room. This will reduce background. (2) The ion guide is 3x longer than the E-36/186 ion guide and 5x longer than the E-317 ion guide giving proportionately better mass resolution. (3) The ion guide is horizontal making surveying more precise and detector changes easier. These two experiments have been designed to fill in some of the gaps left over from the program to date:

(1) A measurement of the real part of the p-d forward scattering amplitude from 8 GeV to ≥ 400 GeV. The p-n real part would be extracted from the data using Glauber theory and compared with measurements of the p-p real part. The highest energy p-n real part measurements reported to date are at 70 GeV.

(2) A remeasurement of the real part of the p-p forward scattering amplitude from 8 GeV to 400 GeV using the same apparatus as the p-d measurements to facilitate the p-p, p-n comparison. By using a long ion guide and position sensitive detectors the accuracy attainable may be significantly improved over previous measurements.²⁰⁾

(3) Measurements of the production of low mass isobars $1.0 < M_x < 2.0$ GeV/c² in the very small momentum transfer region. The mass resolution is given by

$$\Delta M_x = \frac{p\sqrt{|t|}}{M_x} \Delta\theta \quad (13)$$

For example at $p = 200 \text{ GeV/c}$ and $|t| = .02 \text{ (GeV/c)}^2$, the resolution is 10 MeV at the $N^*(1400)$.

(4) Using small-angle proton- He^4 elastic scattering in the $0.1 < |t| < 0.3$ range and at energies ranging continuously from 8 to 500 GeV the Glauber minimum at $|t| \approx 0.24 \text{ (GeV/c)}^2$ will be studied. From this the real part of the nucleon-nucleon scattering amplitude at $|t| \neq 0$ will be extracted using Glauber theory.²¹⁾ In particular, one is interested in knowing if the ratio of the real to the imaginary parts of the nucleon-nucleon scattering amplitude, ρ ($|t| \neq 0$), goes through zero at an energy of 280 GeV as does ρ ($|t| = 0$).

(5) A measurement of the shrinkage in the slope parameter in $p\text{-He}^4$ scattering will also be of interest in view of the difference in α'_{pp} and α'_{pd} commented on above. Azimov et al.¹⁹⁾ predict $\alpha'_{p\text{He}^4} \approx 0.68 \text{ (GeV/c)}^{-2}$.

VI. Conclusions

The program of small-angle low-t "SALT" experiments have as their primary motivation the study of the nucleon-nucleon system. But the use of nuclear targets has been experimentally advantageous and has yielded some nuclear information. The future use of the He^4 target should provide interesting results on both p -nucleon and p -nucleus interactions at high energy.

REFERENCES

*Work supported in part by the U. S. Energy Research and Development Administration, and by the U.S.S.R. State Committee for Atomic Energy.

1) A. C. Melissinos and S. L. Olsen. Physics Reports 17C, 77 (1975). Y. Akimov et al., Zh. Eksp. Theor. Fiz. 48, 767 (1965), (Sov. Phys.--JETP 21, 507 (1965)); Yad. Fiz. 4, 88 (1966), (Sov. J. Nucl. Phys. 4, 63 (1966)).

D. Gross, Ph. D. Thesis, Univ. of Rochester Report No. UR-503, 1974 (unpublished).

2) V. D. Bartenev et al., Phys. Rev. Lett. 29, 1755 (1972).

3) V. D. Bartenev et al., Adv. Cryog. Eng. 18, 460 (1973).

- 4) P. Mantsch and F. Turkot, "Feasibility Study of Gas Jet Target Without Liquid Helium for Use in the Main Ring", Fermilab Report TM-582, June 6, 1975.
P. Mantsch and F. Turkot, "Design of a Gas Jet Target Operating at Ambient Temperature in the Main Ring", Fermilab Report TM-586, June 18, 1975.
- 5) Fermilab Proposal E-198, Rochester-Rutgers-Imperial College Collaboration, "A Proposal for a Magnetic Recoil Spectrometer for the Gas Jet Target", December 21, 1972. Fermilab Proposal E-313: Indiana University, "Polarization in p-p Elastic, Inelastic and Inclusive Reactions at NAL Energies", June 6, 1974.
- 6) Fermilab Proposal E-321: Columbia-Stonybrook Collaboration, "A High Precision Experiment to Measure the Inelastic p-p Cross Section and its Associated Forward Multiplicities at Small Momentum Transfer", June, 1974.
- 7) Fermilab Proposal E-442: Fermilab-Purdue Collaboration, "Study of Nuclear Fragment Emission in Proton Heavy Nucleus Collisions from 10 to 500 GeV/c", September 16, 1975.
- 8) D. Jovanovic, A. Kuznetsov, E. Malamud and V. Nikitin, "Proposal to Expand the NAL Internal Target Area", Fermilab Summer Study, Vol. 1, p. 137, Aug., 1973.
- 9) V. D. Bartenev et al., Phys. Rev. Lett. 31, 1088 (1973).
- 10) V. D. Bartenev et al., Phys. Rev. Lett. 31, 1367 (1973).
- 11) Y. Akimov et al., Phys. Rev. D12, 3399 (1975).
- 12) Y. Akimov et al., Phys. Rev. Lett. 35, 763 (1975);
Y. Akimov et al., *ibid.* 35, 766 (1975).
- 13) Y. Akimov et al., "Analysis of Diffractive $pd \rightarrow Xd$ and $pp \rightarrow Xp$ Interactions and Test of the Finite Mass Sum Rule", Fermilab-Pub-76/36-EXP (to be published).
- 14) Y. Akimov et al., Fermilab Report No. Conf-74/66-EXP (unpublished). Contribution to the XVII International Conference on High Energy Physics, London, 1974.
- 15) The maximum value of M_x^2 for the diffractive process may only be ≈ 0.1 s. But this will only change the constant in equation (10) but not the coefficient of the $\ln s$ rise.
- 16) W. Lockman et al., "Measurement of Total Elastic and Inelastic Diffractive Cross Section and Tests of Factorization at the CERN ISR". University of California, Los Angeles Report 1104. Contribution to the XVIII International Conference on High Energy Physics, Tblisi, USSR, 1976.
- 17) R. E. Hendrick et al., Phys. Rev. D11, 536 (1975) fit σ_{tPP} with the form $4.91 \ln((P_{Lab} + 541)/0.3) + 11.1/P_{Lab}^{0.58}$. A reasonable approximation to the increasing term in the region $100 \leq P_{Lab} \leq 1000$ GeV/c is given by $\Delta\sigma_{tPP} \approx 2.0 \ln s$.

- 18) V. Bartenev et al., Sov. J. Nucl. Phys. 22, 317 (1975).
- 19) Ya. I. Azimov et al., "Diffraction Peak Shrinkage in the Elastic Scattering from Deuteron and the Light Nucleus". Academy of Sciences of the USSR Leningrad Nuclear Physics Institute Report No. 224 (1976) (unpublished).
- 20) V. Bartenev et al., "Measurement of the Real Part of the Proton-Proton Forward Scattering Amplitude from 80 to 280 GeV by Means of Silicon Position Sensitive Detectors". J.I.N.R. report in preparation.
- 21) Measurements of p-He⁴ elastic scattering have been reported by J. Berthot et al. (Clermont-Claude-Bernard-Strasbourg Collaboration). VI International Conference on High Energy Physics and Nuclear Structure. Santa-Fé, New Mexico, June 9-14, 1975. They observe the first Glauber minimum and their preliminary analysis of the data shows no strong t-dependence of ρ .